Engineered *Bacillus subtilis* as oral probiotics to enhance clearance of blood lactate

Mengdi Yang[1,#], Noah Hutchinson[3,#], Ningyuan Ye[3], Jianing Yin[1], Ming Guan[1], Zongqi Wang[3], Peiru Chen[2], Shaobo Yang[1], Justin D. Crane[4], Ke Zhang[1,2], Xuesong He[5,6], Jiahe Li[3]*

[1]Department of Bioengineering, Northeastern University, Boston, MA, 02115, United States.

[2]Department of Chemistry and Chemical Biology, Northeastern University, Boston, MA, 02115, United States.

[3]Department of Biomedical Engineering, University of Michigan, Ann Arbor, MI, 48109, United States.

[4]Internal Medicine Research Unit, Pfizer Inc., 1 Portland Street, Cambridge, MA 02139.

[5]Department of Microbiology, The Forsyth Institute, Cambridge, MA, 02142, United States.

[6]Department of Oral Medicine, Infection and Immunity, Harvard School of Dental Medicine, Boston, MA, 02115, United States.

*Correspondence: Jiahe Li, Department of Biomedical Engineering, University of Michigan, Ann Arbor, MI, 48109, United States. Email: jiaheli@med.umich.edu.

[#] equal contribution

Abstract

Elevated lactate concentrations are implicated in various acute and chronic diseases such as sepsis and mitochondrial dysfunction, respectively. Conversely, ineffective lactate clearance is associated with poor clinical prognoses and high mortality in these diseases. While several groups have proposed using small molecule inhibitors and enzyme replacement to reduce circulating lactate, there are few practical and effective ways to manage this condition. Recent evidence suggests that lactate is exchanged between systemic circulation and the gut, allowing bidirectional modulation between the gut microbiota and peripheral tissues. Inspired by these findings, this work seeks to engineer spore-forming probiotic *B. subtilis* strains to enable intestinal delivery of lactate oxidase as a therapeutic enzyme. After strain optimization, we showed that oral administration of engineered *B. subtilis* spores to the gut of mice reduced elevations in blood lactate in two different mouse models involving exogenous challenge or pharmacologic

perturbation without disrupting gut microbiota composition, liver function, or immune homeostasis. Taken together, through the oral delivery of engineered probiotic spores to the gastrointestinal tract, our proof-of-concept study offers a practical strategy to aid in the management of disease states with elevated blood lactate and provides a new approach to 'knocking down' circulating metabolites to help understand their roles in host physiological and pathological processes.

Significance Statement

This study pioneers the use of engineered *Bacillus subtilis* spores as an oral probiotic therapy to enhance the clearance of elevated blood lactate, a condition linked to severe health issues like sepsis and metabolic disorders. By genetically modifying these spores to deliver therapeutic enzymes directly to the gut, we demonstrated a practical, effective method to modulate systemic lactate levels. This approach leverages the natural exchange between the gut microbiota and systemic circulation, offering a new strategy for managing diseases associated with lactate dysregulation. The safety and efficacy of this method were validated in mouse models, providing a foundation for future clinical applications.

Introduction

Lactate is a hydroxycarboxylic acid and a byproduct of anaerobic glycolysis. When cellular energy demands exceed the rate of oxidative phosphorylation, glycolysis is upregulated to rapidly produce adenosine triphosphate (ATP), and cytosolic pyruvate is converted to lactate by lactate dehydrogenase (LDH) (1). In addition to its role in ATP production, the LDH reaction plays an essential role in the regulation of pH and cellular redox through the oxidization of NADH and the assimilation of protons. Since this reaction is reversible and susceptible to concentration-dependent regulation by its products, the ubiquitous expression of monocarboxylate transporters (MCTs) enables extracellular and systemic lactate concentrations to influence cellular metabolism, acidity and NAD^+/NADH ratios (2) (3). As such, maintaining lactate homeostasis is crucial for the regulation of various biological functions (1). While lactate influxes serve as crucial regulatory signals in many physiologic processes, uncontrolled accumulation of lactate, coined lactic acidosis, can cause physical immobilization, organ failure, hypoxia, and septic shock (4). Further, chronic exposure to elevated lactate concentrations can cause metabolic abnormalities, immune dysregulation (5), hindered wound healing (6), and cellular senescence (2), ultimately contributing to the development of cancer, physical frailty, cardiovascular disease, diabetes, and neurodegeneration (7, 8). Given these implications, strategies to accelerate the clearance of

59 excess lactate and promote the maintenance of healthy blood lactate values possess great utility
60 in the clinical setting. Various lactate-centric treatment methods have been developed, including
61 oxygen therapy (9), intravenous fluid replenishment (10), and medications targeting LDH (11) or
62 lactate transporters (12). However, most of these methods do not directly target lactate itself.

63 Recently, a new strategy was developed that directly mitigates lactic acidosis and intracellular
64 reductive stress by intravenously delivering a dual-enzyme system composed of lactate oxidase
65 (LOX) and *Escherichia coli* catalase (CAT), which irreversibly converts extracellular lactate and
66 oxygen to pyruvate and water (13) (**Figure 1A**). While effective, the direct injection of bacterial
67 enzymes into the bloodstream faces several challenges for translation associated with potential
68 immunogenicity, short serum half-life, and practical considerations such as cost, storage
69 conditions, and difficulties surrounding their requirement for frequent dosing (13). Recent
70 evidence indicates that lactate can freely exchange between peripheral tissues, circulation, and
71 the gut lumen, promoting bidirectional modulation between one another (14-16) (**Figure 1B**). This
72 relationship, combined with bacterial engineering techniques and existing synthetic biology tools
73 can be leveraged through engineered probiotics, which deliver recombinant therapeutic enzymes
74 to the gut for the modulation of systemic lactate. To this end, we have chosen *Bacillus subtilis* as
75 a probiotic candidate for genetic engineering because it is generally recognized as safe (GRAS)
76 by the FDA. Furthermore, *B. subtilis* can form spores, which are associated with improved
77 thermostability, shelf life, and survival in harsh upper gastric conditions to enable germination in
78 the intestine (17).

79 After genomic integration of genes encoding LOX and CAT of various configurations into different
80 *B. subtilis* strains, we performed *in vitro* measurements of peroxide breakdown and lactate
81 consumption to determine the optimal design. Intracellular expression of LOX in *B. subtilis PY79*
82 was capable of efficiently clearing extracellular lactate and thus was chosen for the remainder of
83 the study. Further mouse experiments demonstrated that oral administration of this strain in spore
84 form was effective in not only reducing baseline blood lactate values but also mitigating lactic
85 acidosis following exogenous administration of sodium lactate or inhibition of mitochondrial
86 respiratory chain complex I by metformin. Additional follow-up studies indicated that the
87 introduction of this strain in the mouse gut was safe, transient, and not disruptive to the existing
88 microbial community. These results suggest lactate as a target molecule for efficacious removal
89 with therapeutic potential. More broadly, our work offers an opportunity for probiotics-mediated
90 delivery of therapeutic enzymes in the gut for the modulation of the circulating metabolome.

Results

Genomic integration of genes encoding lactate oxidase and catalase in multiple *B. subtilis* strains

B. subtilis is a Gram-positive, rod-shaped, endospore-forming bacterium isolated from soil, widely utilized for heterologous protein production (18). We initially attempted to produce recombinant enzymes extracellularly by employing the Sec-dependent secretion pathway via fusion with a signal peptide (*amyQ*) in *B. subtilis* WB800N. While WB800N is optimized for extracellular protein production with eight proteases being knocked out, it failed to produce detectable LOX in the supernatant (data not shown). It is possible that LOX (~ 41 kDa as a monomer) can undergo tetramerization to form an even larger protein complex that prohibits efficient protein export, which is one limitation of the Sec-dependent protein secretion pathway (19). Subsequently, our focus shifted to establishing an intracellular expression system by integrating the target gene into a nonessential locus (*amyE*) in the chromosome through homologous recombination (20). To demonstrate the versatility of our approach, we sought to build and test our constructs in four different *B. subtilis* strains including PY79, WB800N, NCIB3610, and HU58 that have been employed for various preclinical trials (20-25). While PY79 and WB800N are amenable to direct transformation of DNA constructs, NCIB3610 and HU58 require phage transduction for genomic integration to allow for stable transgene expression. However, we primarily focused on PY79 in this work due to its widely available genetic information, and proven track record for safety, efficacy, and tractability (24, 26-30).

To enable high-level expression of transgenes from a single copy in the genome, we chose a highly active promoter termed $P_{NBP3510}$ (31). All integration fragments targeting the *amyE* locus consist of three essential components: the *amyE* 5' homologous arm fused with $P_{NBP3510}$, the gene of interest (GOI), and the *amyE* 3' homologous arm coupled with a chloramphenicol resistance selection marker (**Figure 1C**). In pursuit of optimal catalase activity, which is necessary to break down cytotoxic hydrogen peroxide derived from LOX activity, we selected a homologous catalase from *Ureibacillus thermosphaericus*, UtCAT, which is more active and stable than the *E. coli* CAT (32). Various combinations were then created using LOX, UtCAT, and CAT (**Figure 1D**). To couple the expression of UtCAT or CAT with LOX in a single gene cassette, we explored two different configurations. The first strategy is to construct a synthetic operon consisting of the *PNBP3510* promoter with two separate ribosome binding sequences to drive the expression of

123 LOX and UtCAT or CAT, respectively. Two strong RBSs (R0 and B0035), tailored for *B. subtilis*
124 and *E. coli*, were found to be equally active in *B. subtilis* strains. As a result, we generated two
125 strains: *ΔamyE::cat*_LOX_B0035_UtCAT and *ΔamyE::cat*_LOX_R0_UtCAT. In addition to the
126 operon configuration, we also generated fusion proteins, where we inserted a linker peptide (L20)
127 between CAT (UtCAT) and LOX, which was previously designed for intravenous administration
128 of the fusion protein LOXCAT (13). The expression of all constructs was confirmed through
129 Western Blot analysis (**Figure. S1**). Finally, we constructed the integration fragment incorporating
130 the super-folding green fluorescent protein (sfGFP) in various *B. subtilis* strains as negative
131 controls for *in vitro* and *in vivo* lactate clearance measurements (16).

132 **Engineered *B. subtilis* exhibited catalase and lactate oxidase activities as whole-cell**
133 **biocatalysts**

134 The activity of catalase in the CAT and UtCAT strains can be ascertained by monitoring the
135 amount of oxygen gas generated after the direct incubation of engineered strains with hydrogen
136 peroxide as described by others (33). Interestingly, we observed that *B. subtilis* PY79 encoding
137 LOX or sfGFP alone exhibited the ability to break down H_2O_2, and the efficiencies of H_2O_2
138 clearance were comparable to those strains that were engineered to overexpress an additional
139 copy of catalase transgene (the CAT or UtCAT) (**Figure 2A**). Since *B. subtilis* vegetative cells are
140 known to constitutively produce catalases, which confers resistance to oxidative stress[(34)], we
141 speculate that the native catalase activities of *B. subtilis* PY79 were sufficient to degrade H_2O_2, a
142 cytotoxic intermediate from LOX, without the need to overexpress a recombinant catalase.
143 However, it is noteworthy that the endogenous and recombinant catalase activities varied among
144 different *B. subtilis* strains. For instance, no significant improvement of catalase activities was
145 observed in NCIB3610 and HU58 strains that were engineered to overexpress UtCAT or CAT
146 through either a synthetic operon or a genetic fusion configuration, in comparison to those
147 expressing only LOX or sfGFP (**Figure S2**). Conversely, in WB800N, recombinant CAT or UTCAT
148 enhanced catalase activities compared to LOX or sfGFP alone (**Figure S2**). Based on the above
149 findings, we reasoned that expressing a single transgene LOX by itself would be sufficient to
150 safely metabolize lactate without an additional copy of catalase in *B. subtilis*. As homeostatic
151 blood lactate levels are typically < 2 mM, with levels reaching > 4 mM during severe lactic acidosis,
152 we next chose to assess the ability of engineered strains to catabolize lactate *in vitro* with a
153 starting concentration of lactate at 5 mM (35). Notably, PY79 expressing LOX completely removed
154 5 mM L-lactate within 1 hour (**Figure 2B**). To demonstrate the versatility of LOX expression in
155 promoting the degradation of L-lactate, we further engineered three additional *B. subtilis* strains

156 (WB800N, NCIB3610, and HU58) to express LOX, which led to complete breakdown of 5 mM L-
157 lactate within 1-3 hours (**Figure 2C** and **Figure S3**). Based on these findings, we concluded that
158 *B. subtilis* strains expressing intracellular LOX can directly serve as a whole-cell biocatalyst to
159 break down extracellular lactate without the need to use purified recombinant enzymes.

160 **Oral supplementation of engineered *B. subtilis* spores reduced baseline blood lactate and**
161 **accelerated lactate clearance during metabolic challenge**

162 Oral administration of PY79 spores has previously been shown to be safe[(24)], and the spores'
163 superior resistance to extreme conditions could help overcome harsh gastric conditions that
164 diminish the viability of engineered probiotics (36). For these reasons, we further evaluated
165 whether orally administering *B. subtilis* expressing LOX could help mitigate lactic acidosis *in vivo*
166 (**Figure 3A**). Utilizing a published lactate induction model in mice, 6-8 week-old wild type C57BL/6
167 mice were randomly assigned to two groups: *B. subtilis*^{LOX} and *B. subtilis*^{sfGFP}, with *B. subtilis*^{sfGFP}
168 control serving as a bacterial load mimic which does not express LOX. Since a previous safety
169 study in rats did not show clinically significant side effects after a 90-day daily oral administration
170 of 10^{11} CFU/kg body weight engineered PY79 spores (24), we opted to feed the mice with the
171 same dose (~$2x10^9$ CFU per mouse) daily for three days. On Day 3, 20 minutes after the last oral
172 administration of spores, a baseline serum lactate level was measured before we induced
173 experimental lactate elevation. Interestingly, it was found that *B. subtilis*^{LOX} mice displayed lower
174 blood lactate values than *B. subtilis*^{sfGFP} (p=0.02, **Figure 3B**), suggesting that *B. subtilis*^{LOX} could
175 slightly decrease homeostatic blood lactate concentrations. Subsequently, intraperitoneal
176 injection of 2.3 g/kg body weight Na-L-lactate was administered to induce an experimental lactate
177 spike. 30 minutes after injection, *B. subtilis*^{LOX} exhibited less potent increases in blood lactate than
178 that of the sfGFP control group, an effect which persisted through the 75-minute timepoint post-
179 injection before the blood lactate returned to baseline (**Figure 3C**). Of note, *B. subtilis*^{LOX}
180 displayed a significantly reduced area under the curve (AUC, p=0.0027) compared to that of *B.*
181 *subtilis*^{sfGFP} (**Figure 3D**).
182
183 In addition to the exogenous administration of sodium lactate in mice, we further assessed *B.*
184 *subtilis*^{LOX} in a mouse model of drug-induced acute mitochondrial dysfunction using metformin.
185 Metformin is a mitochondrial complex I inhibitor that is known to upregulate serum lactate in
186 humans and mice (35). Utilizing the same gavage schedule as the lactate challenge (**Figure 3A**),
187 mice were administered with an intraperitoneal injection of 400 mg/kg of metformin after the final
188 dose of spores. Blood lactate was measured every 15 minutes between one- and two-hour post-

189 injection. Consistent with the lactate challenge, we observed lower blood lactate values in *B.*
190 *subtilis*^{LOX}-treated mice at 60-, 90-, 105-, and 120-min post-injection (**Figure 3E**), along with a
191 significantly reduced total AUC (p=0.01, **Figure 3F**) in comparison to the *B. subtilis*^{sfGFP} group.
192 Collectively, these findings indicate that oral administration of *B. subtilis*^{LOX} spores can promote
193 resilience to lactic acidosis and/or metabolic challenge in both exogenous lactate challenge and
194 pharmacologic inhibition models.

195 **Oral administration of *B. subtilis* PY79 did not disrupt gut microbiome composition, liver**
196 **function, or immune homeostasis**

197 To understand whether feeding mice with engineered *B. subtilis* strains caused systemic toxicity,
198 blood samples were collected at 0 hour (before oral gavage), 24 hours, 72 hours, and Day 7 after
199 1st oral gavage for different biochemical assays (**Figure 4A**). We found that aminotransferase
200 (ALT) and aspartate aminotransferase (AST) levels in both groups were not significantly different
201 from those in the PBS group (**Figure 4B**). One mouse in the LOX group exhibited an elevated
202 AST level. However, it is important to note that the observed levels for both ALT and AST are
203 considerably lower than the upper limits of the reference ranges for healthy mouse serum, which
204 are 24.3 - 115.25 U/L for ALT and 39.55 - 386.05 U/L for AST (35). In parallel, inflammatory
205 cytokine and chemokine levels were quantified by the Luminex Assay. Compared to the PBS
206 group, administration of *B. subtilis*^{LOX} or *B. subtilis*^{sfGFP} did not elevate representative pro-
207 inflammatory factors including IL-1β, monocyte chemoattractant protein 1 (MCP1) and IFNγ
208 (**Figure 4C**). Other anti-inflammatory and pro-inflammatory cytokine levels were also similar to
209 those in the PBS group (**Figure S4**). Moreover, the concentration of TNFα was extremely low and
210 was undetected in all samples. These findings strongly suggest that feeding *B. subtilis* did not
211 induce any discernible side effects in mice. Subsequently, we assessed whether feeding *B.*
212 *subtilis* would influence the overall composition of the gut microbiome (**Figure 4D**). *B. subtilis* was
213 detected in feces one day after the initial oral gavage and increased with subsequent
214 administrations. However, the total amount of *B. subtilis* reduced 7 days after the first gavage,
215 likely attributed to the cessation of *B. subtilis* administration and the lack of ability to colonize the
216 mouse gut by probiotics in general. By 15 days after the initial gavage, *B. subtilis* was no longer
217 detectable in fecal samples, indicating that *B. subtilis* does not establish long-term colonization in
218 the gut in C57BL/6 mice (**Figure 4E**). Furthermore, there were no discernible differences in
219 colonization between the LOX and sfGFP groups, indicating that the expression of LOX does not
220 likely impact the fitness of *B. subtilis* in the gut (**Figure 4E**). The same stool samples were also
221 collected at the designated time points for 16S rRNA analysis. In terms of relative abundance,

222 *Bacillus* was absent in the top 10 most abundant genera (**Figure S5**). Measures of α-diversity
223 such as Chao1 (**Figure 4F**) or Shannon indices (**Figure S6**) revealed no influence of treatment
224 administered (p=0.488 and 0.16 for Shannon and Chao1, respectively) or time point of sample
225 collection relative to gavage (p=0.137 and 0.67 for Shannon and Chao1, respectively).
226 Additionally, pairwise adonis testing of weighted UniFrac distances between treatment groups
227 across different time points (Day 1, 3, and Day 7) after the first gavage revealed no difference in
228 β-diversity between the LOX, sfGFP and PBS groups (p>0.05) (**Figure 4G**). This indicates that
229 even at relatively low abundance, engineered *B. subtilis* can introduce the functional impact of
230 LOX on blood lactate levels without significantly altering the microbial community in the host.

231 **Discussion**

232 The present work establishes a convenient, safe, and effective method to promote accelerated
233 bodily lactate clearance to manage lactic acidosis. We first determined the optimal design *in vitro,*
234 following which we demonstrated that oral administration of the resultant PY79 strain expressing
235 lactate oxidase led to a safe and transient residence in the fecal microbiota. Functionally, this
236 strain accelerated lactate clearance *in vivo* in experimental models of acute lactic acidosis. Not
237 only is lactic acidosis associated with various chronic conditions such as mitochondrial
238 dysfunction, neurodegeneration, liver disorders and diabetes, it is also considered an indicator for
239 clinical mortalities such as hypoxia, cardiac failure, and sepsis (37-39). Given the reliance on
240 concentration-dependent regulation of the LDH reaction, the removal of lactate and the addition
241 of pyruvate has been proven to alleviate tissue-level reductive stress and promote the assimilation
242 of electrons (13). A technology that can accomplish this through simple oral administration may
243 prove beneficial in acute clinical care, as it circumvents many obstacles associated with
244 environments or dosing needed for other currently approved therapies.

245 Chronically speaking, exposure to elevated lactate concentrations over long periods is associated
246 with the development of various diseases and pathologies. At the cellular level, chronic exposure
247 to elevated lactate has been shown to induce reductive stress, metabolic inflexibility, cellular
248 senescence, and cancer malignancy (40-43). Since elevated blood lactate is purported to
249 represent the mitochondrial status and metabolic flexibility of the respective individual, as
250 previously stated, the clearance of bodily lactate and provision of additional pyruvate may serve
251 to counteract this effect by regulating redox homeostasis through the LDH reaction (13). One
252 limitation of the present work is that the lactate challenges used were merely experimental models
253 with limited external validity. It will be necessary to test more practically relevant metabolic

254 challenge conditions such as treadmill exercise or other models of mitochondrial disease to
255 assess its functional efficacy. Second, blood lactate is the only biochemical outcome measured
256 in this work. It will be important to characterize the effects on not only the metabolome in blood
257 and tissues but also the metabolic and redox status of relevant tissues to unequivocally determine
258 that treatment is conveying a beneficial effect on recipient health and may have a beneficial effect
259 on disease states associated with mitochondrial dysfunction. Given that mitochondrial dysfunction
260 is observed in nearly every significant source of chronic disease-associated mortality, this line of
261 work represents a highly impactful opportunity to help limit healthcare and disease burden from a
262 plethora of sources.

263 In the current work, we chose *B. subtilis* as our chassis not only due to the practical advantages
264 associated with the resistance to harsh gastric conditions and long shelf life of *B. subtilis* spores,
265 but also because oral administration of *B. subtilis* has been demonstrated to have positive impacts
266 on human gut health. For example, it enhances the function of the host immune system, provides
267 protection against infections, and produces nutrients with high bioavailability (44). Additionally, it
268 has previously been used in commercial products, such as Zbiotic, which is a probiotic designed
269 to remove the toxic byproducts of alcohol metabolism (45). Our proof-of-concept work opens
270 possibilities for engineering other bacterial chassis for reducing lactate accumulation, presenting
271 an alternative strategy in sports medicine, metabolic disorders, and gut health. Finally, while we
272 focus on engineering *B. subtilis*, it could provide added benefit to employ other existing bacterial
273 chassis for this purpose such as *E. coli Nissle* and genetically tractable commensal bacteria which
274 can colonize over long periods. Models with transient or long-term colonization present separate
275 advantages from a treatment standpoint and may complement the current model nicely. While it
276 appears that the consumption of extracellular lactate does not require the overexpression of a
277 lactate importer, it remains to be addressed whether the co-expression of a lactate importer may
278 further improve the efficiency of lactate catabolism by facilitating enhanced uptake.

279 In conclusion, we have demonstrated that *B. subtilis* PY79 is a feasible, transient, and safe
280 delivery vessel for therapeutic enzymes, such as lactate oxidase, that achieve targeted
281 modulation of systemic metabolome through its short-term residence in the gut. Additionally, given
282 its ability to form spores that are resilient to harsh conditions and can germinate in the gut, this
283 represents a translatable platform that can be easily stored, delivered, and used for a variety of
284 dosing schedules and pathologies. Due to prior research connecting extracellular lactate on
285 intracellular redox and clinical outcomes, the observed decreases in lactate appear to possess

286 clinically significant potential but warrant further investigation into functional and intracellular
287 outcomes to test this hypothesis.

288 **Materials and Methods**

289 *Chemicals and Reagents*
290 All chemicals and bacterial culture broth were purchased from Fisher Scientific International Inc.
291 (Cambridge, MA, USA) unless otherwise noted, and were of the highest purity or analytical grade
292 commercially available. All molecular cloning reagents including restriction enzymes, competent
293 cells, and the HIFI assembly kit were purchased from New England Biolabs (Ipswich, MA, USA).
294 DNA oligonucleotides were ordered from Sigma Aldrich (St. Louis, MO, USA). LOX, CAT, and
295 UtCAT gblocks were ordered from IDT with *B. subtilis* codon optimization.
296
297 *B. subtilis General Growth Conditions*
298 *B. subtilis* strains were grown at 30°C, 220rpm overnight in LB medium with or without 5ug/mL
299 chloramphenicol. Overnight bacterial culture was diluted 10 times followed by 37°C 220rpm
300 culturing until the OD_{600} reached between 0.6 and 0.8. For *in vivo* studies, bacteria were stored
301 in formulation buffer (2.28g/L KH_2PO_4, 14.5g/L K_2HPO_4, 15% glycerol, pH 7.5) at 10^{11} CFU/mL at
302 -80 °C.
303
304 *Constitutive Strain Construction*
305 All *B. subtilis* strains were constructed in WB800N first. Primers can be found in Supplementary
306 Table 1. All constructs were confirmed by Sanger sequencing.
307
308 All *amyE* locus integration fragments contain three parts: *amyE* 5' arm with $P_{NBP3510}$, GOI, and
309 *amyE* 3' arm with chloramphenicol resistance. The integration fragment was assembled from
310 different plasmids and chromosomal DNA of *B. subtilis* to make *ΔamyE::cat*_sfGFP first which
311 was used as a new template to later make LOX constructs. FLAG and HA tag were added at 3'
312 of LOX and UtCAT respectively. For fusion enzyme CAT_L20_LOX and UtCAT_L20_LOX, FLAG
313 and HA were added at 5' of CAT and 3' of UtCAT respectively.
314
315 *ΔamyE::cat*_sfGFP: The *amyE* 5' arm was amplified through WB800N genomic DNA with the
316 primers B685_V2/B742. $P_{NBP3510}$_sfGFP was amplified from WBSGFP with B741/B747. AmyE 3'
317 arm was amplified through lab plasmid pHT01-NBP3510-sfGFP with B746/B690. Three

318 fragments were first combined through HIFI assembly kit followed by cementing PCR via primers
319 B685_V2/B690 before transformation into *B. subtilis* as described below.
320
321 *ΔamyE::cat* _LOX: *amyE* 5' arm with $P_{NBP3510}$ and with *amyE* 3' arm with Cm^r were amplified by
322 B685_V2/B774 and B776/B690 separately through the chromosomal DNA of PY79
323 *ΔamyE::cat*_sfGFP. LOX was amplified via B775/B777.
324
325 *ΔamyE::cat*_CAT_L20_LOX: *amyE* 5' arm with $P_{NBP3510}$ and *amyE* 3' arm with Cm^r were amplified
326 by B685_V2/B781 and B776/B690 separately through chromosomal DNA of PY79
327 *ΔamyE::cat*_sfGFP. CAT was amplified via B782/B218 through Gblock. LOX was amplified via
328 B218/B783
329
330 *ΔamyE::cat*_LOX_B0035_UtCAT: *amyE* 5' arm with LOX was amplified via B685_V2/B614
331 through chromosomal DNA of PY79 *ΔamyE::cat*_LOX. B0035_UtCAT was amplified via
332 B617/B780 through UtCAT Gblock. *amyE* 3' arms with Cm^r were amplified by B776/B690.
333
334 *ΔamyE::cat*_LOX_R0 _UtCAT: *amyE* 5' arm with LOX was amplified via B685_V2/B778 through
335 chromosomal DNA of PY79 Δ*amyE*::cat_LOX. R0_UtCAT was amplified via B779/B780 through
336 UtCAT Gblock. *amyE* 3' arms with Cm^r were amplified by B776/B690.
337
338 *ΔamyE::cat*_UtCAT_L20 _LOX: *amyE* 5' arm with $P_{NBP3510}$ and *amyE* 3' arm with Cm^r were
339 amplified by B685_V2/B784 and B776/B690 separately through chromosomal DNA of PY79
340 *ΔamyE::cat*_sfGFP. UtCAT was amplified through gblock via B785/B786. L20_LOX was amplified
341 through *ΔamyE::cat*_CAT_L20_LOX via B787/B783.
342
343 *B. subtilis transformation*
344 Cementing PCR products were cleaned up by PB buffer before transformation. MC media was
345 made at a 10x stock with final concentration of 14.036% K_2HPO_4 (w/v), 5.239% KH_2PO_4 (w/v),
346 20% glucose (w/v), 30 mM trisodium citrate, 0.022% Ferric ammonium citrate (w/v), 2% potassium
347 glutamate (w/v), 1% casein digest (Difco). The 10xMC stock was filtered and stored at -20 °C. To
348 make1xMC media, supplemented 1xMC with 3 mM $MgSO_4$. *B. subtilis* strains were re-streaked
349 one day before transformation. Single colonies were inoculated into 1 ml 1xMC media followed
350 by 37 °C, 220rpm shaking for 3-4h until turbid. Cementing PCR products were purified by PB
351 buffer and directly added into 300ul of culture. Culture shaking was resumed at 37 °C for another

352 2.5 h followed by centrifugation to get rid of 250 µL supernatant. The remaining culture was plated
353 on the LB plates with 5 µg/mL Chloramphenicol. Multiple single colonies were picked the next day
354 and restreaked on the selective LB plates to ensure integration. Colonies which grew successfully
355 were picked and verified by Sanger sequencing.
356
357 *SPP1 Phage Transduction*
358 The donor colony was inoculated in 3 mL TY broth (10g tryptone, 5g yeast extract, 5g NaCl per
359 liter) and grew at 37 °C until the culture was turbid. SPPI phage dilutions were prepared from 10^{-}
360 ^{2} to 10^{-6} in sterile tubes. 100 µL of each dilution was added into a clean tube, followed by a 200
361 uL turbid donor culture. Mixtures were incubated statically at 37 °C for 15 mins. TY soft agar (5g
362 agar/L) was melted during the incubation and supplemented with 10 mM $MgSO_4$ and 0.1 mM
363 $MnSO_4$ as working concentration. 3 mL soft agar was added to the bacterial and phage mixture,
364 and the mixture was vortexed. Tube contents were dumped onto the TY agar plate (15g agar/L)
365 and the plate was swirled around to make sure the mixtures covered the entire plate surface.
366 Plates were dried and incubated overnight at 37 °C. The next day lysates were harvested by
367 adding 5 mL TY media to appropriate plaques. Soft agar and TY broth were scraped and
368 incubated at RT for 10 mins, then spun down at 4000 rpm for 15 mins. Lysate was filtered using
369 0.45 µm syringe filter into a new tube and 100 µL chloroform was added for storage. For
370 transduction experiments, lysates were prepared from the donor strains as described above. The
371 recipient colony was inoculated in 3 mL TY broth followed by shaking at 37 °C and 250 rpm until
372 dense.1ml bacterial culture was mixed with 10 µL phage stock followed by adding 9ml TY broth.
373 The mixture was statically incubated at 37 °C in a water bath for 30 mins. The mixture was then
374 centrifuged at 4000 rpm for 20 mins. Most of the supernatant was discarded, and the pellet was
375 resuspended in the remaining volume. 100ul bacterial culture was plated on selective media with
376 10mM sodium citrate. Plates were then incubated overnight at 37 °C. The next day, 3-4 different
377 colonies were restreaked onto selective plates without sodium citrate.
378
379 *Catalase Activity Measurement*
380 Relative catalase activities between different engineered strains were measured and compared
381 by following a previously published protocol (33). Briefly, $1.6x10^{9}$ bacteria were pelleted and
382 resuspended in 100 uL 0.9% NaCl and 100 µL 1% Triton X-100. The solution was transferred to
383 FACS tubes. Subsequently, 100 µL 3% hydrogen peroxide solution (Sigma, catalog #88597-
384 100ML-F) was added to the solution followed by thorough mixing. After the completion of each

385 reaction, the height of the oxygen-forming foam was recorded by subtracting the height of the
386 original solution.
387
388 *Western Blotting*
389 200 uL bacterial pellet was collected by centrifugation and resuspended in 50 µL 1xTE (10mM
390 Tris-HCl, 1 mM EDTA, pH8.0) with 1.5 µL 50mg/ml lysozyme followed by 10 mins incubation in
391 37 °C water bath. 10ul 6xSDS loading dye was added to the suspension. The samples were first
392 separated by 12% SDS-PAGE gel and then transferred to a nitrocellulose membrane (Fisher
393 Scientific). The membranes were incubated with the Anti-FLAG epitope (DYKDDDDK, Biolegend,
394 San Diego, CA, catalog# 637301) or Anti-HA epitope (ABclonal, Woburn, MA catalog# AE008)
395 with 1:2000 dilution overnight in a cold room, and the secondary antibody anti-rat IgG HRP (Cell
396 Signaling Technology, Danvers, MA, catalog# 7077) for Anti-FLAG or anti-mouse IgG HRP
397 (Invitrogen, Waltham, MA, catalog# 626520) for Anti-HA with the same dilution at room
398 temperature for 1 h. Premixed Pierce™ 3,3'diaminobenzidine (DAB) substrate (Fisher Scientific)
399 was used to detect the target proteins.
400
401 *In Vitro Lactate Depletion Measurement*
402 *Bacillus subtilis* LOX, and sfGFP strains were inoculated in LB with 5 µg/mL Cm at 30 °C overnight.
403 Overnight cultures were diluted 10 times into 15 mL fresh LB with 5 µg/mL Cm followed by
404 incubation at 37 °C until OD_{600}=0.8. Pellets were collected by centrifugation at 4000 rpm 20°C for
405 10 mins and washed with PBS three times. 100 uL 0.5 M perchloric acid (PCA) was pre-aliquoted
406 in a 96-well V bottom plate and placed on ice. The pellet was resuspended with PBS and the
407 OD_{600} was adjusted to 1. Bacterial culture and sodium-L-lactate (Fisher, catalog# AAL1450006)
408 standards at concentrations of 5 mM, 2.5 mM, 1.25 mM, 0.625 mM, and 0 mM were added to the
409 corresponding positions of the layout in a 2 mL deep well plate. Sodium-L-lactate was added to
410 the corresponding bacterial suspension with 5 mM working concentration. 100 uL reaction mixture
411 was mixed and transferred to pre-aliquoted PCA on ice as the baseline. The 96-well deep well
412 plate was kept in a shaker at 37 °C 220rpm to collect samples at desired timepoints. The V-bottom
413 plates were spun down at 4 °C 4000rpm for 10 mins after 30mins incubation on ice. 150 uL
414 supernatant was transferred into a new 96-well cell plate and neutralized by 30 µL 2.3M $KHCO_3$
415 followed by overnight precipitation. The plates were centrifuged at 4000rpm 4 °C the next day for
416 10 mins to collect the samples for L-lactate detection. For L-lactate detection, 10 uL of each
417 sample and water blanks were added to 96-flat black well plates with three technical repeats. 185
418 µL LA detection buffer (100 mM Hydrazine dihydrochloride, 100 mM glycine, 0.5 mM NAD^+, pH

419 10) was added to each well followed by 15 mins incubation. The plate was read at excitation 340,
420 emission 460 as the baseline. 5 µL 8U/mL L-Lactic Dehydrogenase (LDH) from rabbit muscle
421 Type II, ammonium sulfate suspension (Sigma L2500) was added to all the wells followed by
422 250rpm shaking for 5 mins to mix well, and plates were kept in the dark. Plates were then
423 incubated in the dark for 2 hours and read.
424
425 *Spore Preparation*
426 Bacterial culture was plated on selective 2xSchaeffer's medium-glucose plates followed by 1-
427 week 37 °C incubation[46]. Spores were scraped from the plate to centrifuge tubes and were then
428 washed by resuspension in ddH_2O. Spores were then pelleted via centrifugation at 5000rpm for
429 10 mins at RT. The pellet was then resuspended in ddH_2O followed by three cycles of 1 min
430 sonication at 20 W and 2,100 Joules, and 1 min rest. Spores were subjected to 1 min sonication
431 followed by 1 min rest. This cycle was repeated step three times a day for 3 days. Spores were
432 aliquoted at 10^9 CFU/mL each tube and stored at -80 °C for later use.
433
434 *In Vivo Lactate Induction Experiments*
435 Five female C57BL/6 mice (Jackson Laboratories) were housed in a single cage for each
436 condition. 6 to 8-week-old mice were gavaged daily with 100 µL containing 10^{11} CFU/kg body
437 weight engineered PY79 spores of the corresponding strain for 3 days. 20 mins after the 3rd oral
438 gavage, baseline blood lactate level was measured by Lactate Plus: Blood Lactate Measuring
439 Meter-Version 2 (NovaBiomedical) and Lactate Plus Meter Test Strips (NovaBiomedical, catalog#
440 40813) through tail snipping. Sodium-L-lactate was administered via intraperitoneal injection at a
441 dose of 2.3 g/kg body weight. Blood lactate was measured 30, 45-, 60-, 75-, and 90-min post
442 injection. For the metformin challenge, 20 mins after the final gavage, baseline blood lactate was
443 measured, and mice were intraperitoneally injected with 400 mg/kg metformin (Fisher Scientific,
444 Waltham MA) in 500 µL PBS. Blood lactate measurements were taken at 60, 75, 90, 105, and
445 120 minutes. Values from both separate experiments are included in the figure containing
446 baseline values (**Figure 3B**).
447
448 *In Vivo Colonization and Safety Experiments*
449 All animal experiments were approved by the University of Michigan and Northeastern University
450 Institutional Animal Care and Use Committee (IACUC). Five female C57BL/6 mice (Jackson
451 Laboratories) were housed in a single cage for each condition. 6 to 8-week-old mice were
452 gavaged daily with PBS or 200 µL engineered *B. subtilis* (10^{10} vegetative cells plus 10^8 spores)

453 for 3 days. Baseline (0h) blood samples were collected into BD Microtainer™ Capillary Blood
454 Collector containing EDTA, right before the 1st oral administration of spores followed by blood
455 collection at 24 h, 72 h, and 7 days post-1st oral gavage. Plasma was isolated by centrifugation at
456 3000xg for 30 mins at 4 °C. The plasma was transferred to clean 0.65 mL tubes for Luminex
457 Assay (MDF10) through Eve Technology (Canada). Plasma was stored in -80 °C until use. AST
458 and ALT levels were sent to the University of Michigan IVAC facility for mini liver chemistry panel
459 (MI1015) analysis. Stools were collected before 1st gavage, and 1 day, 3 days, 5 days, 7 days, 15
460 days, 18 days after 1st gavage. Fecal samples were placed in 300 uL sterile PBS buffer followed
461 by 15 mins incubation. The mixture was homogenized by micro-tissue homogenizer. The solution
462 was obtained by centrifugation and applied to LB agar with 7.5ug/mL chloramphenicol, 0.25ug/mL
463 gentamycin, and 0.25 µg/mL erythromycin. Plates were incubated at 37 °C for 12-16 hours. CFU
464 was determined by standard CFU counting method.
465
466 *Genomic DNA Extraction from Feces*
467 C57BL/6 mouse feces were collected before 1st gavage, and 1 day, 3 days, 5 days, and 7 days,
468 after 1st gavage. Feces were immediately frozen in liquid nitrogen and saved in -80 °C for later
469 use. Genomic DNA was extracted by Quick-DNA Fecal/Soil Microbe Miniprep Kit (Zymo, catalog#
470 D6010) following the instructions.
471
472 *16S rRNA Gene Sequencing and Analysis*
473 16s rRNA analyses were performed both in-house and by Novogene, China. gDNA concentration
474 was measured with 1% agarose gels. According to the concentration, DNA was diluted to 1ng/µL
475 using sterile water. 16S rRNA V4 specific primers are 515F (5'-GTGCCAGCMGCCGCGGTAA-3')
476 and 806A (5'-GGACTACHVGGGTWTCTAAT-3'). All PCR reactions were carried out in 30 µL
477 reactions with 15 µL of Phusion® High-Fidelity PCR Master Mix (New England Biolabs), 0.2 µM
478 of forward and reverse primers, and about 10 ng template DNA. Thermal cycling is started with
479 the initial denaturation at 98°C for 1 min, followed by 30 cycles of denaturation at 98°C for 10 s,
480 annealing at 50°C for 30 s, and elongation at 72°C for 60 s. Finally, within 72°C for 5 min. PCR
481 products were mixed with an equal volume of SYB Green loading buffer and operated
482 electrophoresis on 2% agarose gel for quantification and qualification followed by purification with
483 GeneJET Gel Extraction Kit (Thermo Scientific). Sequencing libraries were generated using NEB
484 Next® Ultra™ DNA Library Prep Kit for Illumina (NEB, USA) following the manufacturer's
485 recommendations and index codes were added. The library quality was assessed on the Qubit@
486 2.0 Fluorometer (Thermo Scientific) and Agilent Bioanalyzer 2100 system. At last, the library was

487 sequenced on an Illumina HiSeq 2500 platform, generating 250 bp paired-end reads. For taxa
488 relative abundance outcomes, qualified reads were filtered by QIIME software to obtain clean
489 tags. All tags were compared with the reference database using UCHIME algorithm to obtain
490 effective tags only which were used for diversity analysis. For diversity analyses, FASTA files
491 were processed with DADA2 for R, with primer sorted and demultiplexed sequences filtered and
492 trimmed at truncation lengths of 240 and 160 bp for forward and reverse reads respectively with
493 a minimum quality score of 20. Following merging and removing of chimeric reads, taxonomy was
494 assigned as Amplicon Sequence Variants (ASVs) with Silva v138 taxonomic database. Using
495 phyloseq for R, ASVs not present at least 5 times in 50% of samples were pruned, and in all
496 outcomes aside from alpha diversity, reads were rarefied to even sampling depth.
497
498 *Statistical Analysis*
499 All statistical analyses were performed using GraphPad Prism 9 (San Diego, CA, USA). Data
500 were analyzed with one-way or two-way analysis of variance (ANOVA) for statistical significance.
501

502 **Acknowledgments**

503 This work was supported by NIBIB (R21EB030769), CDMRP PRMRP (W81XWH-21-1-0016),
504 and in part by NIDCR (R01DE030943). WBSGFP was kindly provided by Prof. Xin Yan from
505 Nanjing Agricultural University, China. SPP1 phage was a generous gift by Professor Dan Kearns
506 from Indiana University Bloomington. We would like to express our gratitude to the ULAM
507 Pathology Core at the University of Michigan for liver panel analyses; Professor Sara Rouhanifard
508 at Northeastern University's Department of Bioengineering for generously sharing her lab's plate
509 reader with us; Professor Ke Zhang at Northeastern University's Department of Chemistry for
510 sharing his lab's equipment and space. We also wish to thank my colleague Morgen Benson for
511 her contribution to the sfGFP construct during the lab rotation.

512 **Conflict of Interest**

513 A provisional patent has been filed by the University of Michigan.

514 **Author contributions**

515 JL conceived the ideas and supervised the experiments. MY designed and conducted the
516 experiments. NH assisted with 16S rRNA α- and β-diversity analysis and conducted experiments

517 validating *in vivo* efficacy. NY assisted with the animal work. JY assisted with material preparation
518 and plate reading for LOX activity *in vitro* tests, as well as phage transduction. MG assisted with
519 spore preparation and western blotting. ZW prepared the *B. subtilis* vegetative cells and assisted
520 in measuring blood lactate. PC provided guidance for mice restraint and blood collection. SY
521 provided guidance for mice oral administration. JC developed the *in vitro* lactate assay. All authors
522 contributed to the discussion of the results and the writing and editing of the manuscript.

523

524 **References**

525 1. Adeva-Andany M, López-Ojén M, Funcasta-Calderón R, Ameneiros-Rodríguez E,
526 Donapetry-García C, Vila-Altesor M, et al. Comprehensive review on lactate metabolism in
527 human health. Mitochondrion. 2014;17:76-100.
528 2. Williamson DH, Lund P, Krebs HA. The redox state of free nicotinamide-adenine
529 dinucleotide in the cytoplasm and mitochondria of rat liver. Biochem J. 1967;103(2):514-27.
530 3. Poole RC, Halestrap AP. Transport of lactate and other monocarboxylates across
531 mammalian plasma membranes. Am J Physiol. 1993;264(4 Pt 1):C761-82.
532 4. Villar J, Short JH, Lighthall G. Lactate Predicts Both Short- and Long-Term Mortality in
533 Patients With and Without Sepsis. Infectious Diseases: Research and Treatment.
534 2019;12:1178633719862776.
535 5. Manosalva C, Quiroga J, Hidalgo AI, Alarcón P, Anseoleaga N, Hidalgo MA, et al. Role of
536 Lactate in Inflammatory Processes: Friend or Foe. Frontiers in Immunology. 2022;12.
537 6. Haller HL, Sander F, Popp D, Rapp M, Hartmann B, Demircan M, et al. Oxygen, pH,
538 Lactate, and Metabolism—How Old Knowledge and New Insights Might Be Combined for New
539 Wound Treatment. Medicina. 2021;57(11):1190.
540 7. Cai M, Wan J, Cai K, Song H, Wang Y, Sun W, et al. Understanding the Contribution of
541 Lactate Metabolism in Cancer Progress: A Perspective from Isomers. Cancers. 2023;15(1):87.
542 8. Steinman MQ, Gao V, Alberini CM. The Role of Lactate-Mediated Metabolic Coupling
543 between Astrocytes and Neurons in Long-Term Memory Formation. Frontiers in Integrative
544 Neuroscience. 2016;10.
545 9. Nørlinger TS, Nielsen PM, Qi H, Mikkelsen E, Hansen K, Schmidt NH, et al. Hyperbaric
546 oxygen therapy reduces renal lactate production. Physiological Reports. 2017;5(6):e13217.
547 10. Rajan S, Srikumar S, Tosh P, Kumar L. Effect of lactate versus acetate-based
548 intravenous fluids on acid-base balance in patients undergoing free flap reconstructive
549 surgeries. Journal of Anaesthesiology Clinical Pharmacology. 2017;33(4):514-9.

550 11. Sada N, Lee S, Katsu T, Otsuki T, Inoue T. Targeting LDH enzymes with a stiripentol
551 analog to treat epilepsy. Science. 2015;347(6228):1362-7.
552 12. Pucino V, Cucchi D, Mauro C. Lactate transporters as therapeutic targets in cancer and
553 inflammatory diseases. Expert Opinion on Therapeutic Targets. 2018;22(9):735-43.
554 13. Patgiri A, Skinner OS, Miyazaki Y, Schleifer G, Marutani E, Shah H, et al. An engineered
555 enzyme that targets circulating lactate to alleviate intracellular NADH:NAD+ imbalance. Nature
556 Biotechnology. 2020;38(3):309-13.
557 14. Fujii T, Nozaki F, Saito K, Hayashi A, Nishigaki Y, Murayama K, et al. Efficacy of pyruvate
558 therapy in patients with mitochondrial disease: A semi-quantitative clinical evaluation study.
559 Molecular Genetics and Metabolism. 2014;112(2):133-8.
560 15. Inoue T, Murakami N, Ayabe T, Oto Y, Nishino I, Goto Y-i, et al. Pyruvate Improved
561 Insulin Secretion Status in a Mitochondrial Diabetes Mellitus Patient. The Journal of Clinical
562 Endocrinology & Metabolism. 2016;101(5):1924-6.
563 16. Scheiman J, Luber JM, Chavkin TA, MacDonald T, Tung A, Pham L-D, et al. Meta-omics
564 analysis of elite athletes identifies a performance-enhancing microbe that functions via lactate
565 metabolism. Nature Medicine. 2019;25(7):1104-9.
566 17. Cho W-I, Chung M-S. Bacillus spores: a review of their properties and inactivation
567 processing technologies. Food Science and Biotechnology. 2020;29(11):1447-61.
568 18. Su Y, Liu C, Fang H, Zhang D. Bacillus subtilis: a universal cell factory for industry,
569 agriculture, biomaterials and medicine. Microbial Cell Factories. 2020;19(1):173.
570 19. Ling Lin F, Zi Rong X, Wei Fen L, Jiang Bing S, Ping L, Chun Xia H. Protein secretion
571 pathways in Bacillus subtilis: Implication for optimization of heterologous protein secretion.
572 Biotechnology Advances. 2007;25(1):1-12.
573 20. Hartl B, Wehrl W, Wiegert T, Homuth G, Schumann W. Development of a new integration
574 site within the Bacillus subtilis chromosome and construction of compatible expression
575 cassettes. J Bacteriol. 2001;183(8):2696-9.
576 21. Piewngam P, Khongthong S, Roekngam N, Theapparat Y, Sunpaweravong S,
577 Faroongsarng D, et al. Probiotic for pathogen-specific Staphylococcus aureus decolonisation in
578 Thailand: a phase 2, double-blind, randomised, placebo-controlled trial. The Lancet Microbe.
579 2023;4(2):e75-e83.
580 22. Piewngam P, Zheng Y, Nguyen TH, Dickey SW, Joo H-S, Villaruz AE, et al. Pathogen
581 elimination by probiotic Bacillus via signalling interference. Nature. 2018;562(7728):532-7.
582 23. Hou Q, Jia J, Lin J, Zhu L, Xie S, Yu Q, et al. Bacillus subtilis programs the differentiation
583 of intestinal secretory lineages to inhibit Salmonella infection. Cell Reports. 2022;40(13):111416.

24. Appala Naidu B, Kannan K, Santhosh Kumar DP, Oliver JWK, Abbott ZD. Lyophilized B. subtilis ZB183 Spores: 90-Day Repeat Dose Oral (Gavage) Toxicity Study in Wistar Rats. Journal of Toxicology. 2019;2019:3042108.

25. Marzorati M, Van den Abbeele P, Bubeck SS, Bayne T, Krishnan K, Young A, et al. Bacillus subtilis HU58 and Bacillus coagulans SC208 Probiotics Reduced the Effects of Antibiotic-Induced Gut Microbiome Dysbiosis in an M-SHIME® Model. Microorganisms. 2020;8(7):1028.

26. Duc LH, Hong HA, Barbosa TM, Henriques AO, Cutting SM. Characterization of Bacillus Probiotics Available for Human Use. Applied and Environmental Microbiology. 2004;70(4):2161-71.

27. Wickramasuriya SS, Park I, Lee Y, Richer LM, Przybyszewski C, Gay CG, et al. Orally delivered Bacillus subtilis expressing chicken NK-2 peptide stabilizes gut microbiota and enhances intestinal health and local immunity in coccidiosis-infected broiler chickens. Poultry Science. 2023;102(5):102590.

28. Hu Y, Miller MM, Derman AI, Ellis BL, Monnerat RG, Pogliano J, et al. Bacillus subtilis Strain Engineered for Treatment of Soil-Transmitted Helminth Diseases. Applied and Environmental Microbiology. 2013;79(18):5527-32.

29. Tam NKM, Uyen NQ, Hong HA, Duc LH, Hoa TT, Serra CR, et al. The Intestinal Life Cycle of Bacillus subtilis and Close Relatives. Journal of Bacteriology. 2006;188(7):2692-700.

30. Cartman ST, Ragione RML, Woodward MJ. Bacillus subtilis Spores Germinate in the Chicken Gastrointestinal Tract. Applied and Environmental Microbiology. 2008;74(16):5254-8.

31. Zhou C, Ye B, Cheng S, Zhao L, Liu Y, Jiang J, et al. Promoter engineering enables overproduction of foreign proteins from a single copy expression cassette in Bacillus subtilis. Microb Cell Fact. 2019;18(1):111.

32. Li G, Lian J, Xue H, Jiang Y, Wu M, Lin J, et al. Enzymatic preparation of pyruvate by a whole-cell biocatalyst coexpressing l-lactate oxidase and catalase. Process Biochemistry. 2020;96:113-21.

33. Iwase T, Tajima A, Sugimoto S, Okuda K, Hironaka I, Kamata Y, et al. A simple assay for measuring catalase activity: a visual approach. Sci Rep. 2013;3:3081.

34. Naclerio G, Baccigalupi L, Caruso C, Felice MD, Ricca E. Bacillus subtilis Vegetative Catalase Is an Extracellular Enzyme. Applied and Environmental Microbiology. 1995;61(12):4471-3.

618 35. Zuniga A, Camacho M, Chang HJ, Fristot E, Mayonove P, Hani EH, et al. Engineered l-
619 Lactate Responding Promoter System Operating in Glucose-Rich and Anoxic Environments.
620 ACS Synth Biol. 2021;10(12):3527-36.
621 36. Luu S, Setlow P. Analysis of the Loss in Heat and Acid Resistance during Germination of
622 Spores of Bacillus Species. Journal of Bacteriology. 2014;196(9):1733-40.
623 37. Wallace DC. A Mitochondrial Paradigm of Metabolic and Degenerative Diseases, Aging,
624 and Cancer: A Dawn for Evolutionary Medicine. Annual Review of Genetics. 2005;39(1):359-
625 407.
626 38. Murphy KF, Balázsi G, Collins JJ. Combinatorial promoter design for engineering noisy
627 gene expression. Proceedings of the National Academy of Sciences. 2007;104(31):12726-31.
628 39. Li X, Yang Y, Zhang B, Lin X, Fu X, An Y, et al. Lactate metabolism in human health and
629 disease. Signal Transduction and Targeted Therapy. 2022;7(1):305.
630 40. Stabenow LK, Zibrova D, Ender C, Helbing DL, Spengler K, Marx C, et al. Oxidative
631 Glucose Metabolism Promotes Senescence in Vascular Endothelial Cells. Cells. 2022;11(14).
632 41. Dou X, Fu Q, Long Q, Liu S, Zou Y, Fu D, et al. PDK4-dependent hypercatabolism and
633 lactate production of senescent cells promotes cancer malignancy. Nat Metab. 2023;5(11):1887-
634 910.
635 42. San-Millan I, Sparagna GC, Chapman HL, Warkins VL, Chatfield KC, Shuff SR, et al.
636 Chronic Lactate Exposure Decreases Mitochondrial Function by Inhibition of Fatty Acid Uptake
637 and Cardiolipin Alterations in Neonatal Rat Cardiomyocytes. Front Nutr. 2022;9:809485.
638 43. Brooks GA. Lactate as a fulcrum of metabolism. Redox Biol. 2020;35.
639 44. Lefevre M, Racedo SM, Ripert G, Housez B, Cazaubiel M, Maudet C, et al. Probiotic
640 strain Bacillus subtilis CU1 stimulates immune system of elderly during common infectious
641 disease period: a randomized, double-blind placebo-controlled study. Immunity & Ageing.
642 2015;12(1):24.
643 45. Lu J, Zhu X, Zhang C, Lu F, Lu Z, Lu Y. Co-expression of alcohol dehydrogenase and
644 aldehyde dehydrogenase in Bacillus subtilis for alcohol detoxification. Food and Chemical
645 Toxicology. 2020;135:110890.
646 46. Ramirez-Peralta A, Zhang P, Li Y-q, Setlow P. Effects of Sporulation Conditions on the
647 Germination and Germination Protein Levels of Bacillus subtilis Spores. Applied and
648 Environmental Microbiology. 2012;78(8):2689-97.
649
650
651
652

653 **Figures and Figure legends**

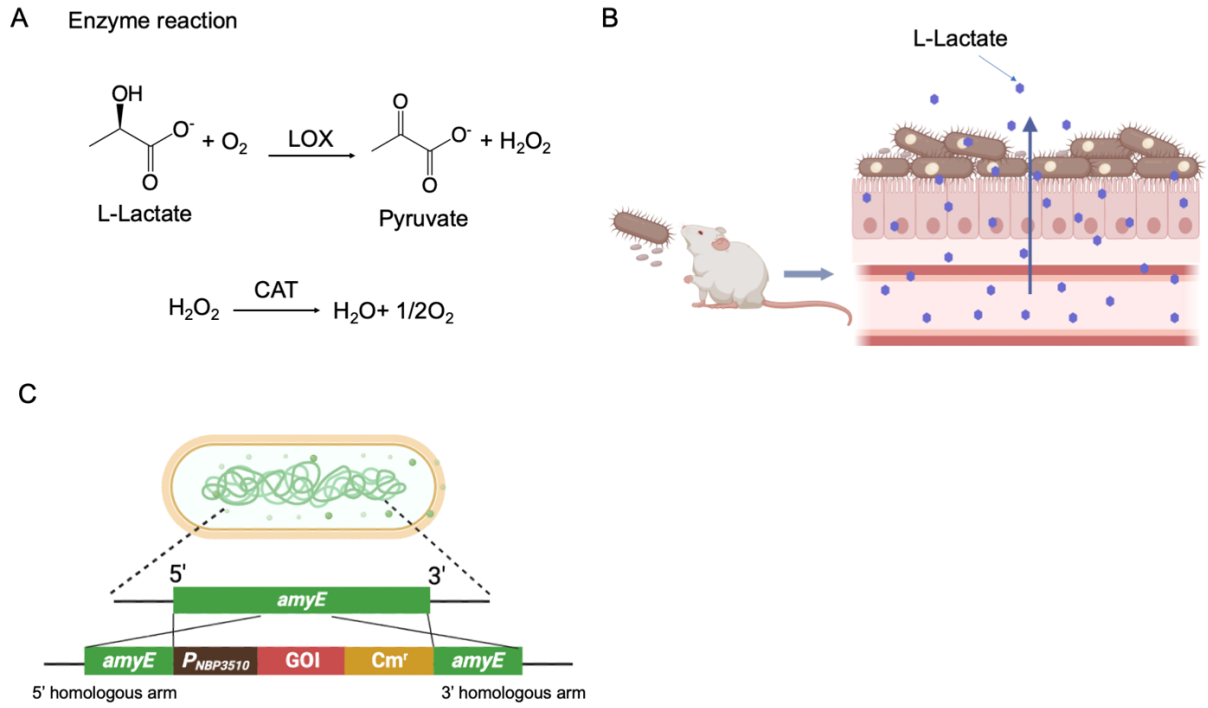

D

Strain List	Gene of Interest (GOI)	Descriptions
1	sfGFP	Negative control strain
2	LOX	Lactate oxidase from *Aerococcus viridans*
3	LOX_R0_UtCAT	R0 is *B. subtilis* derived RBS
4	LOX_B0035_UtCAT	UtCAT is the catalase from *Ureibacillus thermosphaericus* B0035 is *E. coli* derived RBS
5	CAT_L20_LOX	CAT is the catalase from *E. coli*
6	UtCAT_L20_LOX	L20, linker peptide for fusion protein

654

655 **Figure 1. Schematic diagram and genomic integration of lactate oxidase and catalase in**
656 **multiple *B. subtilis* strains.** (A) Enzyme reactions of lactate oxidase (LOX) and catalase (CAT).
657 (B) *B. subtilis* strains were engineered to express lactate oxidase (LOX), facilitating the conversion
658 of lactate to pyruvate. (C) The genetic design involved the incorporation of constitutively
659 expressed transgenes in a nonessential genomic locus such as the *amyE* gene in *B. subtilis*. The
660 gene of interest (GOI) is driven by a constitutive promoter named $P_{NBP3510}$, followed by a
661 chloramphenicol-resistant gene (Cm^r) for selection. The 5' and 3' *amyE* sequences (~1kb in length
662 for each side) are used for homologous recombination. (D) The list of strains used in this study

encodes the following enzymes: LOX (lactate oxidase from *Aerococcus viridans*), CAT (catalase from *E. coli*), and UtCAT (catalase from *Ureibacillus thermosphaericus*). R0 and B0035 are synthetic ribosome binding sequences (RBS). L20, a 20-amino acid peptide linker between two proteins to generate fusion proteins. This figure is created using BioRender.

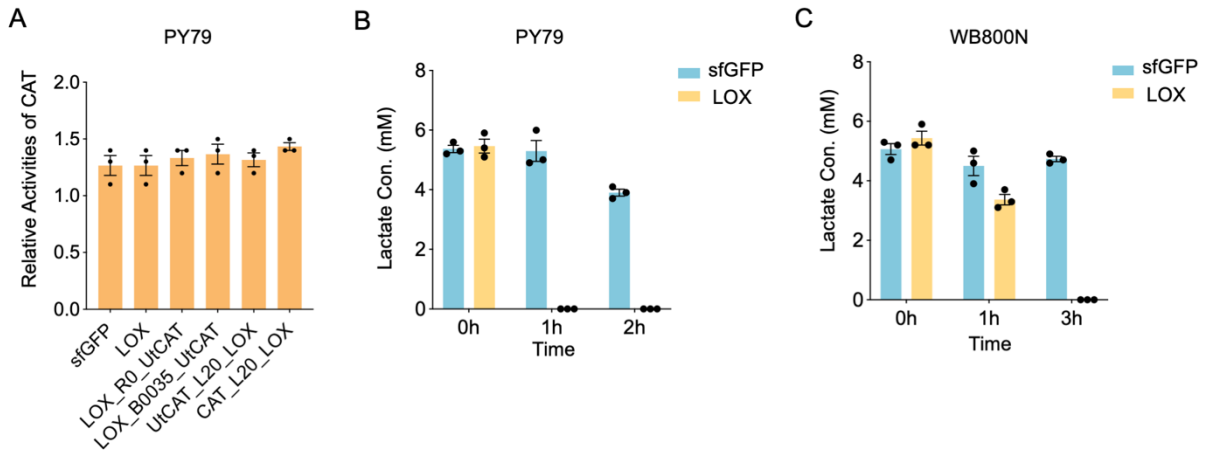

668

669 **Figure 2. *B. subtilis* expressing LOX (*B. subtilis*^{LOX}) exhibited catalase and lactate oxidase**
670 **activities to clear hydrogen peroxide and L-lactate, respectively.** (A) Catalase activities of *B.*
671 *subtilis* PY79 strains encoding different constructs as shown in Figure 1D. *In vitro* lactate
672 consumption of *B. subtilis*^{LOX} in PY79 (B) and WB800N (C) strains from a starting lactate
673 concentration at 5 mM. N=3 independent experiments and n=3 technical replicates.

674

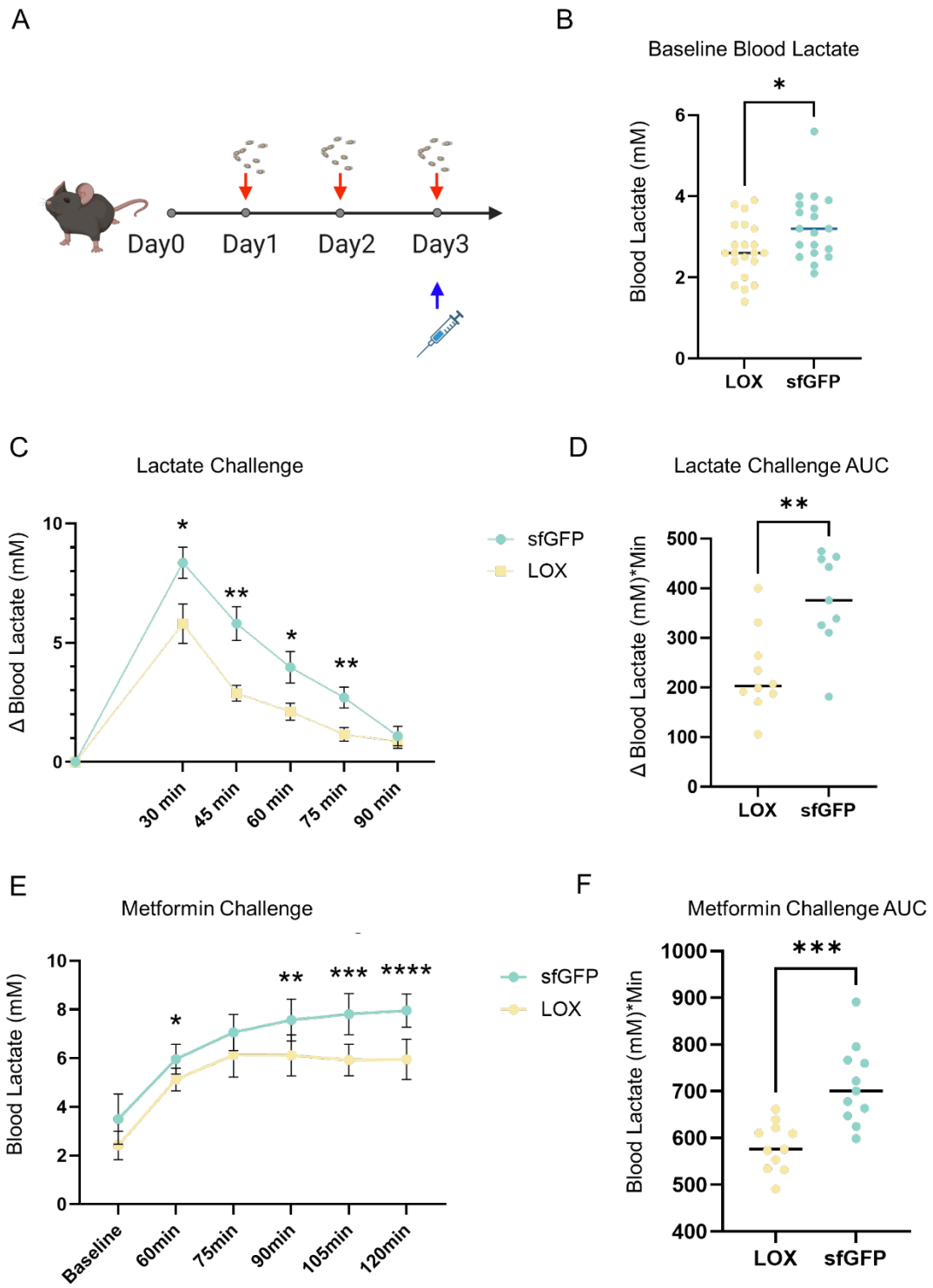

Figure 3. Oral supplementation of *B. subtilis*^{LOX} spores reduced baseline blood lactate and accelerated lactate clearance in two mouse models of metabolic challenge. (A) Schematic diagram of the challenge procedures. After daily oral gavage of spores for three days, L-lactate

679 or metformin was injected intraperitoneally on day 3 to increase blood lactate. (B) Combined
680 baseline blood lactate values prior to challenge in both experiments. n= 21 and 19 for *B. subtilis*^{LOX}
681 and *B. subtilis*^{sfGFP}, respectively. (C) Time course measurements of blood lactate concentration in
682 response to injection of L-lactate. (D) Area Under the Curve (AUC) for blood lactate concentration
683 after injection. n=10 and 9 mice for *B. subtilis*^{LOX} and *B. subtilis*^{sfGFP}, respectively. (E) Time course
684 measurements of blood lactate concentration in response to metformin challenge. (F) AUC for
685 metformin challenge. n=11 and 10 for *B. subtilis*^{LOX} and *B. subtilis*^{sfGFP}, respectively. * $p<0.05$, **
686 $p<0.01$, *** $p<0.001$, **** $p<0.0001$. When not plotted as individual values, data are mean ± SEM.
687 Data were analyzed by student's T test and repeated measures ANOVA followed by pairwise
688 comparisons with the Sidak correction. Δ Blood Lactate=current lactate concentration-baseline
689 concentration.

690
691
692
693
694
695
696
697

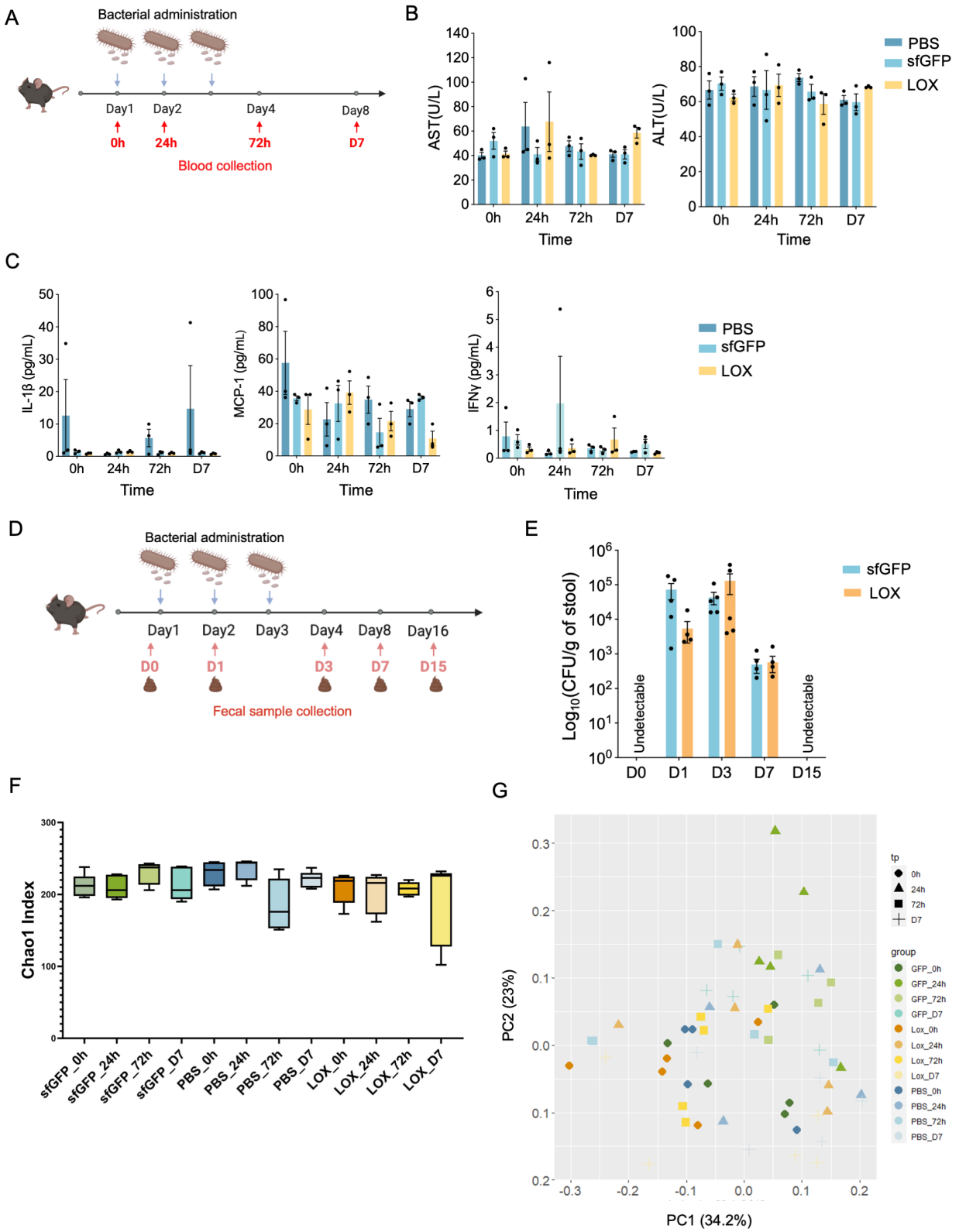

Figure 4. Oral administration of engineered *B. subtilis* PY79 did not disrupt liver function, immune homeostasis, or gut microbiome composition. (A) Schematic of time points for blood

701 collection. “0h” refers to blood samples collected right before the first oral gavage to serve as the
702 baseline. (B) Liver function is represented by circulating ALT and AST levels. ALT and AST
703 concentrations in the plasma of healthy mice range from 24.3 - 115.25 U/L and 39.55 - 386.05
704 U/L respectively. n=3 mice for each treatment. Data are means ± SEM. (C) Concentrations of
705 proinflammatory cytokines and chemokines in mouse plasma. IL, interleukin; MCP, monocyte
706 chemoattractant protein; IFN, interferon. n=3 mice for each treatment. Data are means ± SEM. (D)
707 Schematic of the experimental procedure for oral gavage and fecal sample collection. “D0” refers
708 to fecal samples collected right before the first oral gavage to serve as the baseline. (E) Colony
709 forming unit (CFU) of *B. subtilis* per gram of feces in mice at respective time points. n=5 mice per
710 treatment per time point. (F) Chao1 index of Alpha diversity for respective treatments and time
711 points. n=5 mice for each treatment. (G) Weighted Unifrac Principal Coordinate Analysis (PCoA)
712 found no differences in community composition between different time points or treatment groups.
713 n=5 mice for each treatment, $p > 0.05$.
714